Single Molecule Characterization of α-Synuclein in Aggregation-Prone States

Adam J. Trexler and Elizabeth Rhoades*
Department of Molecular Biophysics and Biochemistry, Yale University, New Haven, Connecticut

ABSTRACT α-Synuclein (αS) is an intrinsically disordered protein whose aggregation into ordered, fibrillar structures underlies the pathogenesis of Parkinson's disease. A full understanding of the factors that cause its conversion from soluble protein to insoluble aggregate requires characterization of the conformations of the monomer protein under conditions that favor aggregation. Here we use single molecule Förster resonance energy transfer to probe the structure of several aggregation-prone states of αS. Both low pH and charged molecules have been shown to accelerate the aggregation of αS and induce conformational changes in the protein. We find that at low pH, the C-terminus of αS undergoes substantial collapse, with minimal effect on the N-terminus and central region. The proximity of the N- and C-termini and the global dimensions of the protein are relatively unaffected by the C-terminal collapse. Moreover, although compact at low pH, with restricted chain motion, the structure of the C-terminus appears to be random. Low pH has a dramatically different effect on αS structure than the molecular aggregation inducers spermine and heparin. Binding of these molecules gives rise to only minor conformational changes in αS, suggesting that their mechanism of aggregation enhancement is fundamentally different from that of low pH.

INTRODUCTION

The functions of intrinsically disordered proteins are conferred by their ability to sample a variety of conformational states in response to changes in cellular environment or upon interactions with cellular binding partners (1). This group of proteins is increasingly associated with a variety of human diseases. Environmental factors that modulate protein conformation have the potential to cause a loss of normal function or confer a toxic gain of function, and may underlie the role of these proteins in disease pathology. Several proteins associated with neurodegenerative amyloid diseases, including β-amyloid and tau in Alzheimer's disease and α-Synuclein (αS) in Parkinson's disease, are representative of this class of proteins; they are disordered under normal physiological conditions, but transition into fibrillar, β-sheet-rich aggregates associated with disease (2). In vitro studies of proteins show that their aggregation is extremely sensitive to solution conditions including pH, salt concentration, organic solvents, and the presence of cofactors (reviewed in (3)). Understanding the conformational changes relevant to the initiation of aggregation requires characterizing the monomer protein under conditions that favor aggregation. However, both their propensity to aggregate under relevant experimental conditions and the innate conformational heterogeneity of intrinsically disordered proteins in solution makes them challenging to study by traditional biophysical and biochemical methods. In recent years, single molecule, Förster resonance energy transfer (smFRET) has begun to prove a useful approach for studying heterogeneous, dynamic denatured states of proteins, including αS (4–10), because it can directly probe unstructured conformations at low concentration that allow for the study of aggregation-prone states without perturbation by intermolecular interactions.

α-Synuclein is a small (14.4 kDa) neuronal protein abundantly expressed in the brain (11). It is the primary component of intracellular amyloid aggregates known as Lewy bodies, the pathological hallmark of Parkinson's disease (PD) (12). PD is characterized by dopaminergic neuronal death, and while the molecular mechanisms underlying cell death are not known, αS appears to play a central role (13). The native function of αS is thought to involve synaptic vesicle maintenance or recycling (14,15), and defects in vesicle trafficking are observed when αS is overexpressed in a variety of model organisms (16–19).

α-Synuclein has three regions (Fig. 1): the N-terminus contains repeats of the conserved KTKEGV motif that mediates binding to anionic lipids; the central NAC region, residues ~61–95, is hydrophobic and thought to be responsible for aggregation; and the C-terminus is highly negatively charged. Although αS is unstructured in solution at neutral pH (20,21), upon binding to lipid membranes or membrane mimetics, the first 100 residues form an amphipathic α-helix, while the C-terminus remains largely disordered (20). The geometry of this α-helical stretch seems to be dependent on the membrane curvature and lipid composition; detergent micelles with a high degree of curvature enforce a bent helical conformation, while αS adopts a single extended helix on larger lipid vesicles (22–28).

Because of their importance in understanding the initiation of aggregation, there is tremendous interest in elucidating the structures of aggregation-prone states of αS. Both NMR and ensemble fluorescence studies of αS at physiological pH found evidence of long-range contacts between the N- and

Submitted July 19, 2010, and accepted for publication August 27, 2010.

*Correspondence: elizabeth.rhoades@yale.edu

Editor: Patricia L. Clark.

0006-3495/10/11/3048/8 $2.00

doi: 10.1016/j.bpj.2010.08.056

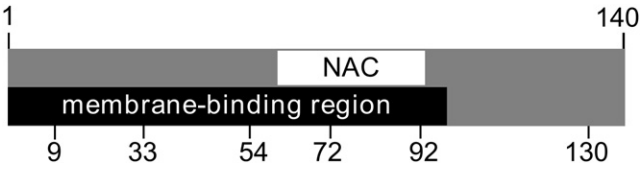

FIGURE 1 Schematic of αS primary structure. αS is divided into three regions: the N-terminal membrane binding region (residues 1–100), a central hydrophobic, NAC region (61–95), and the highly acidic C-terminal region (95–140). Positions of residues mutated to cysteines for smFRET labeling in this study are labeled.

C-termini, as well as between the C-terminus and the NAC region, leading to the hypothesis that long-range interactions may act to shield the central, more hydrophobic region of αS (29–31). Subsequently, it was suggested that disruption of these long-range interactions, observed at low pH or upon binding of polycationic molecules, increases the solvent exposure of the NAC region, resulting in accelerated fibrillation (29,32). Alternatively, it has been proposed that aggregation is induced by charge neutralization of the C-terminus, resulting in its compaction and a consequent increase in hydrophobic contact with the NAC region (32–34).

Here we use smFRET to study aggregation-prone states of αS. We find that at low pH the C-terminus of αS is compact and in close proximity to the NAC region. Monitoring the denaturation of the low pH state reveals that it undergoes a coil-globule unfolding transition, with evidence of restricted chain motion in the collapsed state. In order to look for common structural motifs in aggregation-prone states, we investigate the ability of charged molecular aggregation inducers, spermine and heparin, to cause conformational changes in αS. Intriguingly, we observe no evidence that spermine or heparin binding results in appreciable structural changes to αS. While both low pH and polyions have been shown to accelerate αS aggregation, our results show that the mechanisms by which these work are fundamentally different.

MATERIALS AND METHODS

Protein expression, purification, and labeling

α-Synuclein was expressed from a T7-7 plasmid in *Escherichia coli* BL21 cells. Purification was performed as described previously (20,24). To prevent the possible misincorporation of a cysteine at position Y136 (35), a conservative mutation (TAC to TAT) was made in all variants of αS utilized here. Single and double cysteine mutants of αS were made to allow for site-specific attachment of maleimide reactive fluorophores on the cysteines (Fig. 1). For FRET measurements, Alexa Fluor 488 maleimide and Alexa Fluor 594 maleimide (Invitrogen, Carlsbad, CA) were used for the donor and acceptor dyes, respectively; this fluorophore pair is expected to have a Förster radius, the distance at which the probability of energy transfer is 50%, of ~54 Å (36). α-Synuclein was labeled sequentially, first with acceptor fluorophore, followed by donor fluorophore, under conditions based on the manufacturer's instructions, as described previously (24) (details in the Supporting Material). As a control, we confirmed that fluorophore labeling of αS does not significantly disrupt binding to lipid vesicles (approximately twofold change in binding affinity, dependent upon label placement (24,37)) or incorporation of the labeled protein into fibrillar aggregates (details in the Supporting Material).

Data collection and analysis

Measurements were made in eight-well chambered cover glasses (Nunc, Rochester, NY) that were treated by incubation with polylysine-conjugated polyethylene glycol to prevent αS from adsorbing to chamber surfaces (24). Labeled αS was diluted into 20 mM Tris buffer with 140 mM NaCl at pH 7.4 or 3.0 to a final concentration of ~90 pM. For denaturation experiments, an 8 M stock of guanidine hydrochloride (GdnHCl) in water was diluted into Tris buffer. Heparin, spermine, and dithiodiethylcarbamate (DDC) were purchased from Sigma (St. Louis, MO) and used without further purification. Stocks were made in water and diluted into buffer (final concentrations: 300 μM spermine, 500 nM heparin, and 100 μM DDC, concentrations that have been shown to accelerate αS aggregation) before measurement.

SmFRET measurements were made on a home-built system that has been described previously (24) (instrument details in the Supporting Material). Fluorescence emission from labeled αS was collected in 1-ms time bins from diffusing proteins and the photons were split into donor and acceptor channels. To discriminate photon bursts arising from protein transit through the focal volume from background noise, we employed a threshold scheme by selecting the number of photons at which the highest signal/noise ratio was obtained. This threshold was calculated by comparing photon traces of buffer in the absence and presence of protein. We employed a sum (sum of counts in the donor and acceptor channels) threshold to discriminate protein events from background and an acceptor threshold to eliminate the zero-peak, a well-known artifact of diffusion-based smFRET measurements (details of threshold analysis in the Supporting Material).

The energy transfer efficiency, ET_{eff}, is calculated for each protein burst by

$$I_a/(I_a + \gamma^* I_d),$$

where I_a and I_d are the number of photons collected in the acceptor and donor channels, respectively, corrected for signal bleedthrough, and γ is a correction factor which accounts for quantum yield and detection efficiency differences (details in the Supporting Material). Under the conditions of our measurement, the background signal was negligible with average counts of $\ll 1$ photon per time bin. For each sample, several thousand protein events were measured, and ET_{eff} was calculated for each event and compiled into a histogram for further analysis. For all constructs used, at least two different sets of measurements were analyzed separately, to ensure their reproducibility. Histograms shown here are either combined datasets to increase the number of total events in the histogram, or representative single datasets. On average, each histogram consists of >4000 protein transit events.

Steady-state anisotropy and fluorescence lifetimes of single labeled αS constructs were used to probe the rotational freedom and local environment of the fluorophores. The hydrodynamic radii of these constructs were measured with fluorescence correlation spectroscopy (FCS) (experimental details in the Supporting Material).

RESULTS

In smFRET, changes in distance between two fluorophores can be measured by changes in the calculated ET_{eff} (38). This direct readout is a powerful approach for measuring conformational changes in unstructured proteins such as αS. Many changes in intramolecular distance that accompany secondary or tertiary structure rearrangements are directly measurable by smFRET, but are inaccessible or difficult to interpret using traditional structural techniques.

While ET_{eff} can be converted to distance via the Förster equation (38,39) or other models (6,36), there are a variety of inherent difficulties with this conversion, and we prefer to rely primarily on relative changes in ET_{eff} to measure differences in αS structure as a function of solution conditions.

Low pH ($\leq$3.0) has been shown to induce partial structure in αS and concomitant acceleration of amyloid fibril formation (40), leading to the suggestion that it is an appropriate model for characterizing the conformational changes of αS relevant to aggregation (32,40). In order to investigate the conformations of αS at low pH, we first measured ET_{eff} of αS constructs designed to probe the C-terminal domain and central region of the protein (Fig. 2). One fluorophore was placed at residue 130, which serves as a fixed point in the C-terminus (shown previously not to perturb normal protein structure and function (24)), and the second fluorophore was placed throughout the protein. SmFRET

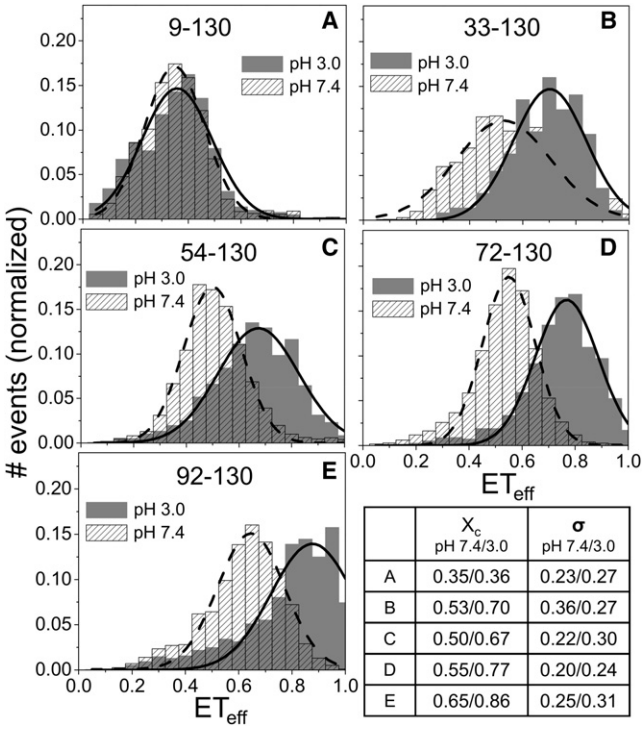

	X_c pH 7.4/3.0	σ pH 7.4/3.0
A	0.35/0.36	0.23/0.27
B	0.53/0.70	0.36/0.27
C	0.50/0.67	0.22/0.30
D	0.55/0.77	0.20/0.24
E	0.65/0.86	0.25/0.31

FIGURE 2 Collapse of the C-terminus of αS at low pH. (*A–E*) ET_{eff} histograms for αS double mutants, labeling sites displayed in each panel. (*Solid lines*) Gaussian fits to the ET_{eff} distribution. Panels *B–E* show that the mean values of the histograms (x_c) shift to higher values at low pH, indicating a decrease in the separation between the C-terminus and the central (~30–100) region of the protein. Panel *A* shows that, in contrast to other regions of the protein, there is very little change in the distance between the N- and C-termini at neutral and low pH. FCS measurements support this finding, as the ratio of average αS diffusion time at pH 3.0 to pH 7.4 is 0.98 (by the Student's *t*-test, $p = 0.001$, no significant difference). Although smFRET and FCS are sensitive to different dimensional properties, radius of gyration and hydrodynamic radius, respectively, both measurements indicate that the global dimensions of αS at pH 7.4 and 3.0 are similar. (*Lower right-hand panel*) Summary of the mean values (x_c) and full width at half-maximum (σ) taken from the Gaussian fits of all constructs at both pHs.

measurements between residue 130 and residues 33, 54, 72, and 92 show that the C-terminal region undergoes substantial compaction at pH 3.0 (Fig. 2, *B–E*). To determine the extent of the pH-induced structural changes, we measured constructs designed to probe the N-terminus and NAC region, with donor and acceptor fluorophores placed at residue pairs 9–54, 33–72, 54–72, and 72–92. The ET_{eff} histograms show small differences between pH 7.4 and pH 3.0 (Fig. S2 in the Supporting Material), indicating that the compaction is localized to the C-terminus, while the N-terminus and NAC region remain relatively unchanged. The C-terminal compaction shown in Fig. 2 was not dependent upon probe placement at position 130, as a similar degree of compaction was observed for αS labeled at residue 140 (data not shown).

Moreover, compaction of the C-terminus does not appear to affect the relative proximity of the N- and C-termini of the protein. For a construct labeled at residues 9 and 130, the ET_{eff} histograms at pH 7.4 and 3.0 are comparable, suggesting that the end-to-end distances are similar between the physiological and low pH states (Fig. 2 *A*). This smFRET data is supported by FCS measurements of αS at pH 7.4 and pH 3.0, which show that the diffusion times, proportional to hydrodynamic radius, measured at both pH values are identical within experimental error (see Fig. 2 legend and the Supporting Material for details). This finding is in very good agreement with a pulse-field gradient NMR measurement of αS, which found comparable hydrodynamic radii at pH 7.4 and 3.0 (32).

Steady-state fluorescence anisotropy measurements were used to verify that the fluorophores retained similar rotational freedom under both pH conditions and at all labeling positions (Table S1). Alexa Fluor 488 gave an average anisotropy (value averaged over six labeling positions, shown in Fig. 1) of 0.07 ± 0.02 at pH 7.4 and 0.08 ± 0.02 at pH 3.0. Alexa Fluor 594 gave larger average anisotropy values, 0.11 ± 0.01 at pH 7.4 and 0.13 ± 0.03 at pH 3. The anisotropy values reflect fluorophore, segmental, and whole protein rotation, and the slight increase at low pH may be due to a loss of regional flexibility upon compaction of the protein. However, even the larger anisotropy values are not expected to cause significant artifacts in the ET_{eff} calculations (8,41), and are very similar to those previously reported for these dyes used in smFRET studies (6,8,27,42,43).

Fluorescence lifetime measurements of both αS labeled with either Alexa Fluor 488 or Alexa Fluor 594 at all six labeling positions were made (Table S1). The lifetime of Alexa Fluor 594 (4.4 ns ± 0.03 ns) was remarkably stable regardless of its labeling position or pH. We noted more, though still very little, variability in Alexa Fluor 488 lifetime (average lifetime 4.0 ns ± 0.25). Specifically, the lifetime of Alexa Fluor 488 at residue 130 was the most significantly affected, with an ~10% contribution of a second exponential decay in the lifetime distribution. We attribute this to the presence of several nearby tyrosine residues

(at positions 125, 133, and 136), which are known to quench Alexa Fluor 488 (44).

Because we are characterizing conformational changes in the monomer protein that are relevant to the initiation of aggregation, it was important to ensure that the aggregation behavior of αS was not severely impacted by the presence of the fluorophores. We used double-labeled versions of all five mutants shown in Fig. 2 (details in the Supporting Material) to show that fluorescently labeled protein was incorporated into the aggregates, which supports the idea that the fluorescently labeled protein is capable of sampling aggregation-relevant states. Together with the lifetime and anisotropy measurements, these results strongly suggest that the fluorophores do not interact significantly with nearby side chains or hydrophobic regions of the protein. These fluorophores have been used for several studies of αS, as well as other intrinsically disordered and folded proteins, and generally they have not been found to perturb protein structure or function (6,9,23,27,45).

To determine whether there were common structural features relevant to the acceleration of αS aggregation, we used smFRET to measure the effects of three different classes of molecular aggregation enhancers on the structure of αS. Both polycations and polyanions have been shown to accelerate αS aggregation (46,47), and spermine and heparin, respectively, were chosen as representative molecules of these classes. A third type of inducer (48,49), the pesticide DDC, which was suggested to act on αS primarily via a non-charge-dependent mechanism, was also chosen. Upon incubation with spermine, heparin, or DDC, we measured only very slight shifts in the ET_{eff} histogram peaks for probes of the C-terminus, N-terminus, and NAC regions of αS (Fig. 3 and Fig. S3). An excess of all three molecules, several orders-of-magnitude greater than the concentration of αS, were used to ensure saturation of all binding sites on the protein. Although very small, reproducible shifts in ET_{eff} peak values (<0.05 ET_{eff} units) were observed for some regions of αS upon incubation with some of the aggregation inducers (Fig. 3 and Fig. S3) and were suggestive of slight conformational changes, these were not nearly as dramatic as the pH-induced changes (Fig. 2).

The nature of the conformational change that results in compaction of the C-terminus at pH 3.0 was further probed by characterizing denaturation of the low pH state (Fig. 4). For a construct labeled at residues 72 and 130 (Fig. 2 *D*), increasing concentrations of GdnHCl resulted in only a single peak in the ET_{eff} histogram that shifted to lower mean ET_{eff} values (Fig. 4). There was no increase in the widths of the ET_{eff} distributions for concentrations of GdnHCl <3 M (Table S2). Unfolding transitions studied by smFRET can differ dramatically based on the nature of the initial native state. The unfolding transition for globular proteins monitored by smFRET is well studied (36,50,51). As denaturant concentration is increased, two populations are observed in ET_{eff} histograms, one peak corresponding to the folded subpopulation and one peak corresponding to the unfolded subpopulation. For coil-globule transitions, on the other hand, the ET_{eff} histogram generally shows

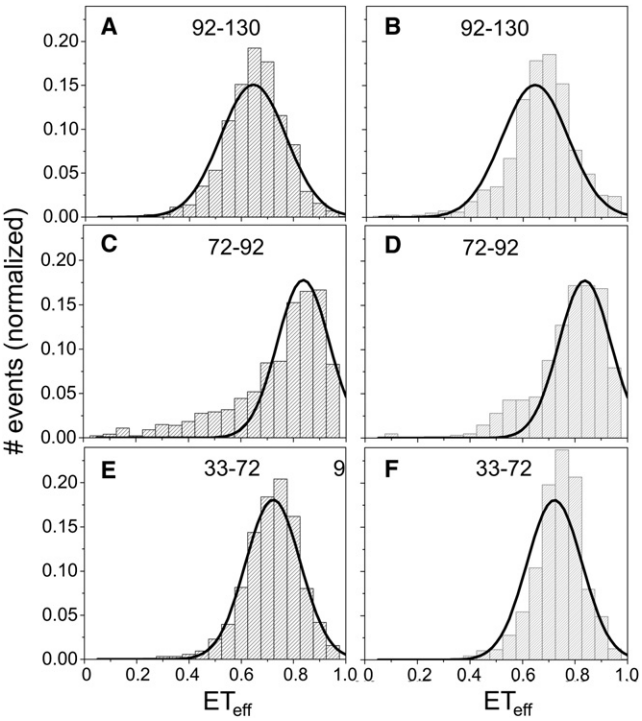

FIGURE 3 Effects of aggregation inducers on conformation of αS. (*A*, *C*, and *E*) Spermine (300 μM) causes only minor conformational changes throughout αS, as seen by slight shifts in the ET_{eff} histograms for constructs probing the C-terminus, NAC region, and N-terminus, respectively, in the presence (*columns*) and absence (*solid lines*) of spermine. (*B*, *D*, and *F*) Heparin (500 nM) shows similar results for the same αS constructs. For comparison, the solid lines in each panel are a Gaussian fit to the same αS construct in pH 7.4 buffer in the absence of molecular aggregation inducers.

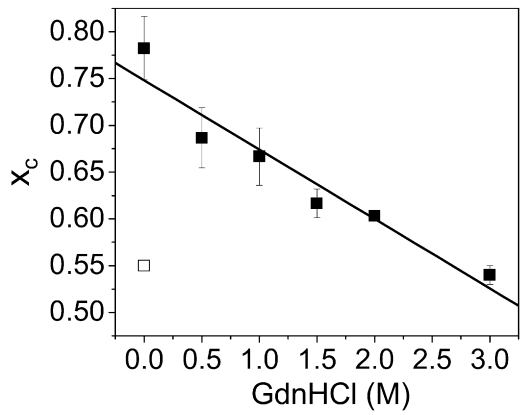

FIGURE 4 Denaturation of the low pH state monitored by smFRET. Solid squares are mean value, x_c, from the Gaussian fit to the ET_{eff} histogram for αS-labeled at residues 72 and 130, measured at pH 3.0 with increasing concentrations of GdnHCl. Error bars are standard deviation of three experiments on three separate labeling preparations. (*Open square*) Mean value of the ET_{eff} histogram of the same αS construct at pH 7.4. The widths of the Gaussian fits to the ET_{eff} histograms were invariant up to 3 M GdnHCl (Table S2).

only a single peak—corresponding to a random coil population, which shifts to lower ET_{eff} values as the molecule expands with increasing denaturant concentration (7,9). Our data are consistent with a denaturant-induced expansion of a random structure, suggesting that the low pH, aggregation-prone conformation of αS is not a canonical globular fold, but instead a collapsed, random state. The absence of broadening in the ET_{eff} distributions at intermediate GdnHCl concentrations suggests that only a single population is sampled. Rebinning the data or collecting with smaller time bins (100–200 μs), which should resolve subpopulations blurred by relatively slow (on the timescale of diffusion) conformational interchange, did not produce evidence of multiple populations at intermediate concentrations of GdnHCl. A polyproline peptide was used for control measurements (45) to ensure that changes in the measured ET_{eff} were not due to viscosity or refractive index differences (data not shown).

DISCUSSION

Effect of pH and molecular inducers on conformation of αS

In this study, we used smFRET to probe the pH-induced collapse of the C-terminus of αS and compare the effects of pH with those caused by interactions with molecular aggregation inducers. Because contact between the C-terminus and the N-terminus of αS has been suggested to inhibit aggregation (29,30), we were particularly interested in determining how collapse of the C-terminus at low pH affected its interactions with the NAC and N-terminal regions of the protein. Our data show that at pH 3.0 the C-terminus of αS collapses and comes in close proximity to the NAC domain, as seen by large shifts in the peak positions of the ET_{eff} histograms (Fig. 2, *B–E*). It is important to note that while the increase in ET_{eff} distribution widths at low pH may be attributed to dynamics (see below), the shifts of the mean values of the histograms indicate that the structural change in the C-terminus between pH 7.4 and pH 3.0 is stable, not due to transient sampling of structures. The high degree of similarity between the ET_{eff} histograms at pH 3.0 and pH 7.4 of the construct labeled at positions 9 and 130 (Fig. 2 *A*) suggests that a relatively close proximity of the termini is found at both pH values, despite the significant compaction of the C-terminus at pH 3.0. (Fig. 5). Our findings are consistent with several recent NMR reports showing that the end-to-end contacts of αS as measured by paramagnetic relaxation enhancement are comparable at neutral and low pH (32–34). It was suggested that global dimensions of the protein may be relatively unchanged due to a compensatory expansion of the N-terminus upon collapse of the C-terminus (32).

In contrast to the dramatic changes induced by low pH, binding of molecular aggregation accelerators spermine and heparin had only minor effects on the protein conformation. Heparin is thought to bind positively charged lysine residues located throughout the N-terminus of αS, and it has been suggested that it may accelerate aggregation by stabilizing transient β-sheet structure in this region (47). Although smFRET does not report directly on secondary structure, stable or transient β-sheet structure would be expected to increase the distance between the probe residues, or decrease the ET_{eff}. The small changes we observe indicate a shift to a higher $ET_{eff,}$ or more compact structure, in both the N- and C-termini (Fig. 3, *B* and *F*). Spermine, on the other hand, binds to a well-defined site on the C-terminus of αS (52). No discernable effect on the conformation of αS was seen upon spermine binding (Fig. 3, *A*, *C*, and *E*).

Our results present a striking contrast to several previous reports. A recent mass spectrometry/ion mobility study showed spermine causes an almost twofold compaction of αS (53), and two NMR reports found subtle, global conformational changes throughout residues 22–93 (52) as well as

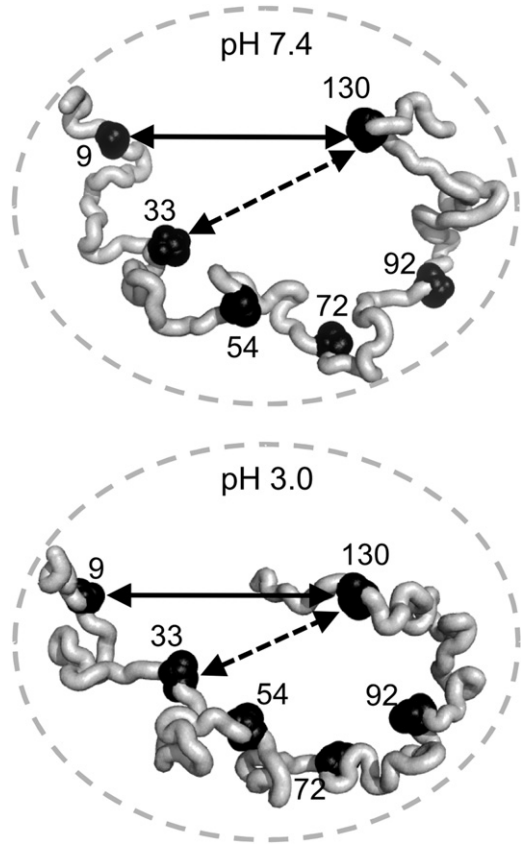

FIGURE 5 Cartoon highlighting differential distance changes between residues 9–130 and 33–130 at pH 7.4 and 3.0. The solid arrows, which span residues 9–130, are the same size in both figures, whereas the dashed arrow, between residues 33–130, in the pH 3.0 figure is shorter than the dashed arrow in the pH 7.4 figure, reflecting the relative closer proximity between these two residues at pH 3.0. The circles are also the same size in both figures, indicating that the overall dimensions of the protein remain the same at both pH values (based on our FCS measurements and the hydrodynamic radius measurements from other groups).

disruption of N- to C-terminal contacts and an expansion of the C-terminus (29). It is possible that smFRET, which lacks the residue-level resolution of NMR, is insensitive to these conformational changes. However, we are able to detect subtle conformational changes in αS (<0.05 ET_{eff} units) upon heparin binding (Fig. 3, *B* and *F*) and upon αS denaturation (Fig. 4). It is possible that in ensemble measurements, although generally done under conditions that should inhibit aggregation, the significantly higher protein concentrations required (for instance, ~100 μM used in NMR compared to ~100 pM used in smFRET) could result in intermolecular interactions that favor structural changes. When 50 nM labeled αS was incubated with increasing concentrations of unlabeled αS at pH 3.0, aberrant autocorrelation curves, usually indicative of aggregation (54), were observed by FCS when the total protein concentration reached ~10 μM (data not shown). At 50 μM unlabeled protein, the average diffusion time of αS began to increase, suggesting that the population of larger species was significant enough to cause a shift in the average size of the protein population. These observations suggest that the higher concentrations used for ensemble studies may result in the presence of small populations of aggregated states that could complicate interpretation of monomer structures.

Mechanism of aggregation enhancement

Because pH causes an obvious compaction of the C-terminus and spermine also binds to the C-terminus, this work highlights the importance of the C-terminus in controlling the aggregation of αS. Based on our observations, we conclude that the conformational changes αS undergoes at low pH are fundamentally different than those it undergoes as a result of binding to spermine, and thus the mechanism by which aggregation is induced is also fundamentally different. However, as neither spermine binding nor low pH results in significant conformational changes in the NAC region or disruption of N- to C-terminal interaction, we do not find evidence that either mechanism of aggregation enhancement is the result of increased solvent exposure of the NAC region due to the disruption of long-range contacts (29). Our pH 3.0 data is more consistent with two recent NMR studies which propose that at low pH, compaction of the C-terminus allows for the juxtaposition of hydrophobic residues from the C-terminus and NAC region into a larger hydrophobic cluster capable of driving aggregation (33,34). This collapse is hypothesized to be driven by charge neutralization in the C-terminus. However, simply using high concentrations of NaCl, which also enhances αS aggregation (55,56), to screen the charges in the C-terminus does not induce collapse as observed at low pH, but results, instead, in a slight expansion of this region (Fig. S4). This finding correlates well with our observation that charge neutralization by spermine does not induce collapse of the C-terminus (Fig. 3 *A*)—leading us to propose that simple hydrophobic collapse, allowed in the absence of electrostatic repulsions in the C-terminus, may not be sufficient for compaction. Rather, at low pH the charge distribution of the C-terminus is dramatically altered from that at neutral pH (−13.2 at pH 7.4 to +1.0 at pH 3.0 for residues 101–140) such that charge is effectively removed from the C-terminus, which clearly results in compaction of this region, increasing the intramolecular contacts within the protein (Fig. 2, *B–E*). Spermine is expected to shield the negative charges of the C-terminus, but not eliminate them. This shielding does not, in our measurements, result in significant conformational changes in αS (Fig. 3, *A*, *C*, and *E*). From this data, we suggest that the mechanism of aggregation enhancement by spermine, as well as by other ionic inducers, may act to enhance aggregation by reducing electrostatic repulsion between protein molecules, and thus increasing intermolecular association, without requiring formation of the hydrophobic core found at low pH.

The nature of the C-terminus at low pH

It has been suggested that a general model for the initiation of aggregation of amyloidogenic proteins is through self-association via hydrophobic domains exposed by partial folding/unfolding (2). For disordered αS, this mechanism necessitates chain collapse, such as we observe at low pH. This state may share many features of molten globules (3), well known from protein folding, where it has been used to describe states with a high degree of secondary structure and little or no tertiary structure, as well as compact states with indeterminate secondary structure (40,57). While we cannot assign secondary structure with smFRET, we observe a high degree of compaction in the C-terminus of αS at pH 3.0 (Fig. 2). NMR reports on the effect of low pH on the structure of the C-terminus are mixed (34), although evidence of an increase in α-helical content of this region has been reported (32,33). Furthermore, the unfolding of the low pH state of αS is more similar to the coil-globule transition seen in the unfolded population in single molecule folding studies (6,7,9) as opposed to a two-state unfolding suggested by the presence of an isosbestic point in circular dichroism data (40).

A molten-globule-like state is expected to limit the configurational space of the protein, slowing the dynamics of the protein chain. In this context, it is notable that the ET_{eff} histograms for constructs reporting on the C-terminus structure of αS are generally wider at pH 3.0 than those at pH 7.4 (Fig. 2). While there are a number of factors which contribute to the width of smFRET histograms (45,58), an increase can be indicative of slowing in the polypeptide chain dynamics (59,60), as would be expected in a molten-globule-like state. Indeed, slow dynamics (>200 μs) have been observed in the molten globule states found in pH denatured apomyoglobin (61). Further supporting this idea is an NMR study showing an increase in the rigidity of the C-terminus at low pH (32), as well as the small, but consistent, increase in the anisotropy

of the fluorophores at the majority of the labeling sites at pH 3.0, likely a reflection of decreased flexibility of the polypeptide chain (41,62). The implication of a molten-globule-like state on the pathway to aggregation is that the slow conformational rearrangements expected in this state disfavor an intermolecular association mechanism that requires the formation of specific structure, and favors one wherein initial intermolecular interactions are between random, collapsed states. Several recent articles aimed at characterizing the structure of the oligomeric structures formed early in the aggregation pathway show that they are largely disordered (63,64).

CONCLUSIONS

In this study, we have shown that αS undergoes a dramatic compaction in the C-terminal region at low pH. This structure does not appear to be a general conformation responsible for acceleration of αS aggregation, as we have observed that neither heparin nor spermine (charged molecules that accelerate aggregation) induce such large-scale conformational changes in αS. This suggests that the mechanism by which heparin and spermine accelerate αS aggregation is via charge neutralization, not by enhancing or inducing partial folding in αS, as has been previously suggested. We have found the low pH collapsed state has predominantly random tertiary interactions, supporting the hypothesis that this state resembles a molten globule. Given that the association of monomer αS into oligomeric species may be one of the first pathological events in PD, our results highlight the power of single molecule measurements in elucidating the molecular mechanisms underlying this fundamental process.

SUPPORTING MATERIAL

Four figures and two tables are available at http://www.biophysj.org/biophysj/supplemental/S0006-3495(10)01052-0.

We thank Dr. Eva Sevcsik and Elizabeth Middleton for reading and commenting on the manuscript.

We gratefully acknowledge financial support from the Ellison Medical Foundation (to E.R.), the Beverly and Raymond Sackler Institute for Biological, Physical, and Engineering Sciences (to E.R.), and an institutional training grant from the National Institutes of Health (No. GM007223 to A.J.T.).

REFERENCES

1. Uversky, V. N., C. J. Oldfield, and A. K. Dunker. 2008. Intrinsically disordered proteins in human diseases: introducing the D2 concept. *Annu. Rev. Biophys.* 37:215–246.
2. Chiti, F., and C. M. Dobson. 2006. Protein misfolding, functional amyloid, and human disease. *Annu. Rev. Biochem.* 75:333–366.
3. Uversky, V. N. 2008. Amyloidogenesis of natively unfolded proteins. *Curr. Alzheimer Res.* 5:260–287.
4. Chen, H., and E. Rhoades. 2008. Fluorescence characterization of denatured proteins. *Curr. Opin. Struct. Biol.* 18:516–524.
5. Schuler, B., and W. A. Eaton. 2008. Protein folding studied by single-molecule FRET. *Curr. Opin. Struct. Biol.* 18:16–26.
6. Merchant, K. A., R. B. Best, …, W. A. Eaton. 2007. Characterizing the unfolded states of proteins using single-molecule FRET spectroscopy and molecular simulations. *Proc. Natl. Acad. Sci. USA.* 104: 1528–1533.
7. Sherman, E., and G. Haran. 2006. Coil-globule transition in the denatured state of a small protein. *Proc. Natl. Acad. Sci. USA.* 103:11539–11543.
8. McCarney, E. R., J. H. Werner, …, K. W. Plaxco. 2005. Site-specific dimensions across a highly denatured protein; a single molecule study. *J. Mol. Biol.* 352:672–682.
9. Mukhopadhyay, S., R. Krishnan, …, A. A. Deniz. 2007. A natively unfolded yeast prion monomer adopts an ensemble of collapsed and rapidly fluctuating structures. *Proc. Natl. Acad. Sci. USA.* 104: 2649–2654.
10. Ferreon, A. C., C. R. Moran, …, A. A. Deniz. 2010. Alteration of the α-synuclein folding landscape by a mutation related to Parkinson's disease. *Angew. Chem. Int. Ed. Engl.* 49:3469–3472.
11. George, J. M., H. Jin, …, D. F. Clayton. 1995. Characterization of a novel protein regulated during the critical period for song learning in the zebra finch. *Neuron.* 15:361–372.
12. Spillantini, M. G., R. A. Crowther, …, M. Goedert. 1998. α-Synuclein in filamentous inclusions of Lewy bodies from Parkinson's disease and dementia with Lewy bodies. *Proc. Natl. Acad. Sci. USA.* 95: 6469–6473.
13. Cookson, M. R. 2005. The biochemistry of Parkinson's disease. *Annu. Rev. Biochem.* 74:29–52.
14. Chandra, S., F. Fornai, …, T. C. Südhof. 2004. Double-knockout mice for α- and β-synucleins: effect on synaptic functions. *Proc. Natl. Acad. Sci. USA.* 101:14966–14971.
15. Abeliovich, A., Y. Schmitz, …, A. Rosenthal. 2000. Mice lacking α-synuclein display functional deficits in the nigrostriatal dopamine system. *Neuron.* 25:239–252.
16. Cooper, A. A., A. D. Gitler, …, S. Lindquist. 2006. Alpha-synuclein blocks ER-Golgi traffic and Rab1 rescues neuron loss in Parkinson's models. *Science.* 313:324–328.
17. Gitler, A. D., B. J. Bevis, …, S. Lindquist. 2008. The Parkinson's disease protein α-synuclein disrupts cellular Rab homeostasis. *Proc. Natl. Acad. Sci. USA.* 105:145–150.
18. Nemani, V. M., W. Lu, …, R. H. Edwards. 2010. Increased expression of α-synuclein reduces neurotransmitter release by inhibiting synaptic vesicle reclustering after endocytosis. *Neuron.* 65:66–79.
19. Thayanidhi, N., J. R. Helm, …, J. C. Hay. 2010. Alpha-synuclein delays endoplasmic reticulum (ER)-to-Golgi transport in mammalian cells by antagonizing ER/Golgi SNAREs. *Mol. Biol. Cell.* 21: 1850–1863.
20. Eliezer, D., E. Kutluay, …, G. Browne. 2001. Conformational properties of α-synuclein in its free and lipid-associated states. *J. Mol. Biol.* 307:1061–1073.
21. Davidson, W. S., A. Jonas, …, J. M. George. 1998. Stabilization of α-synuclein secondary structure upon binding to synthetic membranes. *J. Biol. Chem.* 273:9443–9449.
22. Jao, C. C., B. G. Hegde, …, R. Langen. 2008. Structure of membrane-bound α-synuclein from site-directed spin labeling and computational refinement. *Proc. Natl. Acad. Sci. USA.* 105:19666–19671.
23. Veldhuis, G., I. Segers-Nolten, …, V. Subramaniam. 2009. Single-molecule FRET reveals structural heterogeneity of SDS-bound α-synuclein. *ChemBioChem.* 10:436–439.
24. Trexler, A. J., and E. Rhoades. 2009. Alpha-synuclein binds large unilamellar vesicles as an extended helix. *Biochemistry.* 48:2304–2306.
25. Jao, C. C., A. Der-Sarkissian, …, R. Langen. 2004. Structure of membrane-bound α-synuclein studied by site-directed spin labeling. *Proc. Natl. Acad. Sci. USA.* 101:8331–8336.
26. Ulmer, T. S., A. Bax, …, R. L. Nussbaum. 2005. Structure and dynamics of micelle-bound human α-synuclein. *J. Biol. Chem.* 280: 9595–9603.

27. Ferreon, A. C., Y. Gambin, …, A. A. Deniz. 2009. Interplay of α-synuclein binding and conformational switching probed by single-molecule fluorescence. *Proc. Natl. Acad. Sci. USA.* 106:5645–5650.
28. Drescher, M., B. D. van Rooijen, …, M. Huber. 2010. A stable lipid-induced aggregate of α-synuclein. *J. Am. Chem. Soc.* 132:4080–4082.
29. Bertoncini, C. W., Y. S. Jung, …, M. Zweckstetter. 2005. Release of long-range tertiary interactions potentiates aggregation of natively unstructured α-synuclein. *Proc. Natl. Acad. Sci. USA.* 102:1430–1435.
30. Dedmon, M. M., K. Lindorff-Larsen, …, C. M. Dobson. 2005. Mapping long-range interactions in α-synuclein using spin-label NMR and ensemble molecular dynamics simulations. *J. Am. Chem. Soc.* 127:476–477.
31. Lee, J. C., H. B. Gray, and J. R. Winkler. 2005. Tertiary contact formation in α-synuclein probed by electron transfer. *J. Am. Chem. Soc.* 127: 16388–16389.
32. Cho, M. K., G. Nodet, …, M. Zweckstetter. 2009. Structural characterization of α-synuclein in an aggregation prone state. *Protein Sci.* 18:1840–1846.
33. McClendon, S., C. C. Rospigliosi, and D. Eliezer. 2009. Charge neutralization and collapse of the C-terminal tail of α-synuclein at low pH. *Protein Sci.* 18:1531–1540.
34. Wu, K. P., D. S. Weinstock, …, J. Baum. 2009. Structural reorganization of α-synuclein at low pH observed by NMR and REMD simulations. *J. Mol. Biol.* 391:784–796.
35. Masuda, M., N. Dohmae, …, M. Hasegawa. 2006. Cysteine misincorporation in bacterially expressed human α-synuclein. *FEBS Lett.* 580:1775–1779.
36. Schuler, B., E. A. Lipman, and W. A. Eaton. 2002. Probing the free-energy surface for protein folding with single-molecule fluorescence spectroscopy. *Nature.* 419:743–747.
37. Middleton, E. R., and E. Rhoades. 2010. Effects of curvature and composition on α-synuclein binding to lipid vesicles. *Biophys. J.* 99, 2279–2188.
38. Forster, T. 1948. Intermolecular energy migration and fluorescence. *Ann. Phys. (Berlin).* 2:55–75.
39. Stryer, L. 1978. Fluorescence energy transfer as a spectroscopic ruler. *Annu. Rev. Biochem.* 47:819–846.
40. Uversky, V. N., J. Li, and A. L. Fink. 2001. Evidence for a partially folded intermediate in α-synuclein fibril formation. *J. Biol. Chem.* 276:10737–10744.
41. Lakowicz, J. 2006. Principles of Fluorescence Spectroscopy. Springer, New York, NY.
42. Mukhopadhyay, S., and A. A. Deniz. 2007. Fluorescence from diffusing single molecules illuminates biomolecular structure and dynamics. *J. Fluoresc.* 17:775–783.
43. Rhoades, E., E. Gussakovsky, and G. Haran. 2003. Watching proteins fold one molecule at a time. *Proc. Natl. Acad. Sci. USA.* 100: 3197–3202.
44. Chen, H., S. S. Ahsan, …, W. W. Webb. 2010. Mechanisms of quenching of Alexa fluorophores by natural amino acids. *J. Am. Chem. Soc.* 132:7244–7245.
45. Schuler, B., E. A. Lipman, …, W. A. Eaton. 2005. Polyproline and the "spectroscopic ruler" revisited with single-molecule fluorescence. *Proc. Natl. Acad. Sci. USA.* 102:2754–2759.
46. Antony, T., W. Hoyer, …, V. Subramaniam. 2003. Cellular polyamines promote the aggregation of α-synuclein. *J. Biol. Chem.* 278: 3235–3240.
47. Cohlberg, J. A., J. Li, …, A. L. Fink. 2002. Heparin and other glycosaminoglycans stimulate the formation of amyloid fibrils from α-synuclein in vitro. *Biochemistry.* 41:1502–1511.
48. Uversky, V. N., J. Li, and A. L. Fink. 2001. Pesticides directly accelerate the rate of α-synuclein fibril formation: a possible factor in Parkinson's disease. *FEBS Lett.* 500:105–108.
49. Uversky, V. N., J. Li, …, A. L. Fink. 2002. Synergistic effects of pesticides and metals on the fibrillation of α-synuclein: implications for Parkinson's disease. *Neurotoxicology.* 23:527–536.
50. Deniz, A. A., M. Dahan, …, P. G. Schultz. 1999. Single-pair fluorescence resonance energy transfer on freely diffusing molecules: observation of Förster distance dependence and subpopulations. *Proc. Natl. Acad. Sci. USA.* 96:3670–3675.
51. Rhoades, E., M. Cohen, …, G. Haran. 2004. Two-state folding observed in individual protein molecules. *J. Am. Chem. Soc.* 126:14686–14687.
52. Fernández, C. O., W. Hoyer, …, T. M. Jovin. 2004. NMR of α-synuclein-polyamine complexes elucidates the mechanism and kinetics of induced aggregation. *EMBO J.* 23:2039–2046.
53. Grabenauer, M., S. L. Bernstein, …, M. T. Bowers. 2008. Spermine binding to Parkinson's protein α-synuclein and its disease-related A30P and A53T mutants. *J. Phys. Chem. B.* 112:11147–11154.
54. Nath, S., J. Meuvis, …, Y. Engelborghs. 2010. Early aggregation steps in α-synuclein as measured by FCS and FRET: evidence for a contagious conformational change. *Biophys. J.* 98:1302–1311.
55. Hoyer, W., D. Cherny, …, T. M. Jovin. 2004. Impact of the acidic C-terminal region comprising amino acids 109–140 on α-synuclein aggregation in vitro. *Biochemistry.* 43:16233–16242.
56. Munishkina, L. A., J. Henriques, …, A. L. Fink. 2004. Role of protein-water interactions and electrostatics in α-synuclein fibril formation. *Biochemistry.* 43:3289–3300.
57. Uversky, V. N., and O. B. Ptitsyn. 1994. "Partly folded" state, a new equilibrium state of protein molecules: four-state guanidinium chloride-induced unfolding of β-lactamase at low temperature. *Biochemistry.* 33:2782–2791.
58. Nir, E., X. Michalet, …, S. Weiss. 2006. Shot-noise limited single-molecule FRET histograms: comparison between theory and experiments. *J. Phys. Chem. B.* 110:22103–22124.
59. Gopich, I. V., and A. Szabo. 2007. Single-molecule FRET with diffusion and conformational dynamics. *J. Phys. Chem. B.* 111: 12925–12932.
60. Michalet, X., S. Weiss, and M. Jäger. 2006. Single-molecule fluorescence studies of protein folding and conformational dynamics. *Chem. Rev.* 106:1785–1813.
61. Chen, H., E. Rhoades, …, W. W. Webb. 2007. Dynamics of equilibrium structural fluctuations of apomyoglobin measured by fluorescence correlation spectroscopy. *Proc. Natl. Acad. Sci. USA.* 104: 10459–10464.
62. Cantor, C. R., and P. R. Schimmel. 1980. Biophysical chemistry. *In* Part II: Techniques for the Study of Biological Structure and Function. W.H. Freeman and Company, New York.
63. Wu, K. P., and J. Baum. 2010. Detection of transient interchain interactions in the intrinsically disordered protein α-synuclein by NMR paramagnetic relaxation enhancement. *J. Am. Chem. Soc.* 132:5546–5547.
64. Bhak, G., J. H. Lee, …, S. R. Paik. 2009. Granular assembly of α-synuclein leading to the accelerated amyloid fibril formation with shear stress. *PLoS ONE.* 4:e4177.